Cite this article
Farajniya R and Poursorkhabi RV (2025)
Specialised impounding plan of a rockfill dam after construction case study of Madani dam.
Geotechnical Research **12(2)**: 102–112,
https://doi.org/10.1680/jgere.24.00050

Research Article
Paper 2400050
Received 29/05/2023; Accepted 28/12/2024

Geotechnical Research

Specialised impounding plan of a rockfill dam after construction case study of Madani dam

Rasoul Farajniya MSc
PhD Candidate, Department of Civil Engineering, Tabriz Branch, Islamic Azad University, Tabriz, Iran

Ramin Vafaei Poursorkhabi PhD
Associate Professor, Department of Civil Engineering, Tabriz Branch, Islamic Azad University, Tabriz, Iran; Robotics and Soft Technologies Research Center, Tabriz Branch, Islamic Azad University, Tabriz, Iran (corresponding author: raminvafaei@yahoo.com)

To control and ensure the safety of the Madani Tabriz dam at the period 10 years after the end of construction, dam monitoring is performed utilising data from the instrumentation installed on the dam's body. In this study, using the Midas finite element software, the results of the settlement, pore water pressure, and total stress of the Madani rockfill dam were calculated 10 years after the end of construction of the dam body and compared with the results of the instrumentation observation. The linear correlation coefficients between the data obtained from the sensors and the numerical analysis results for the items of settlement, pore water pressure, and total stress are 84%, 67%, and 99%, respectively. Sensitivity analyses were carried out for present special impounding programme for the dam, with controlling two simultaneous items: the pore water pressure and effect stress changes in the clay core, with 10 years passed since the completion of construction of the dam body. While controlling the reliability coefficient of the body stability, with a 30 cm/d reservoir impounding, the dam reservoir will be filled in 80 d. Suggest an impounding program for a reservoir behind an earth or rockfill dam, detailing a specific plan that ensures all safety aspects of the dam are controlled.

Keywords: impounding/monitoring/pore water pressure/rockfill dam/settlement/stress

Notation

A	settlement at a given level
A_{max}	maximum settlement observed in the dam body
c	material adhesion or cohesion
E	modulus of elasticity of materials
H	level at which settlement, stress, or pore pressure is measured
H_{max}	maximum dam crown level
K	permeability coefficient
P	pore water pressure
P_{max}	maximum pore water pressure
R_u	arching ratio
v	poisson's ratio
Y	relative change of settlement to maximum settlement
z	installation elevation of instruments
γ_d	dry specific gravity
γ_{sat}	saturated specific gravity
Δ	settlement at a specific level
σ	total stress
σ_{max}	maximum total stress
φ	internal friction angle

1. Introduction

Monitoring involves checking the dam's performance at the end of the construction and operation phases and ensuring compliance with design predictions. The International Commission on Large Dams recommends continuous monitoring of dam safety and stability during construction and operation (Blind, 1983; Cheng *et al*., 2021). Monitoring is achieved by installing appropriate instruments in sensitive areas to measure various parameters, such as pore water pressure, deformation, and total stress (Liu *et al*., 2023). The increased pore water pressure within the dam body reduces effect stress and, consequently, decreases the shear strength of the dam materials, which can lead to dangerous outcomes, such as embankment instability (Ghiasi *et al*., 2021; Komasi and Beiranvand, 2019). The amount of saturated settlement in the upstream shell of the dam caused by the first impounding of the reservoir can be determined using data recorded by the dam body sensors (Khalili-Maleki *et al*., 2022; Soroush and Aghaei Araei, 2006). The stability of rockfill dams can be estimated using numerical modelling, which is crucial for controlling the stability of dams against natural disasters (earthquakes, floods, and landslides), poor design, and inadequate maintenance (Farajniya *et al*., 2022; Sivasuriyan *et al*., 2021). The factor of safety obtained from numerical analyses must fall within the allowable range for controlling the stability of dam body slopes (Ghaemi and Konrad, 2022; Zhenyu *et al*., 2020). Heterogeneous settlement can occur between different parts of the dam, know n as 'arching' leading to cracks in the impermeable cross-section of the dam body (clay core), especially near the supports, due to the differing properties of core and shell materials. These cracks can expand during reservoir impoundment due to the pressure exerted on the core, potentially leading to the hydraulic failure of the dam body (Beiranvand and Komasi, 2019). Rockfill dam cores have been evaluated for hydraulic failure through laboratory tests and numerical analyses, suggesting the use of GM–GC rather than CL materials for rockfill dam cores (Behrouz Sarand *et al*., 2023;

Ghanbari and Shams, 2015). Studies indicate that maximum long-term settlement typically occurs in the middle of the dam core (Mazaheri *et al*., 2020). In addition, it has been reported that 88% of total dam settlement occurs during construction (Rashidi and Haeri, 2017; Zareh *et al.*, 2023). One study found that settlement decreases and eventually stabilises over time after the first reservoir impounding, even as the reservoir volume increases (Guo *et al*., 2018; Zhou *et al*., 2011). The results of studies conducted thus far indicate that numerical analysis is one of the methods for assessing the stability of rockfill dams. Sole reliance on stability analyses without comparison with results from other methods, such as dam body monitoring, is not a reliable approach. Therefore, this study focuses on the Madani Tabriz dam, which took a decade to construct and has been completed for 10 years. To date, no comprehensive study has been conducted on controlling the stability factors of the dam body. Consequently, the stability of the dam body has been assessed concurrently with numerical analysis results and data from precision instrumentation. Furthermore, the correlation coefficients between numerical analysis results and instrumentation data for the three stability factors of the dam body vertical settlement, pore water pressure variations, and total stress were examined. Finally, the impounding of the reservoir for this specific dam should not be carried out solely based on conventional codes. Instead, a specialised reservoir impounding plan should be developed according to the dam body conditions, based on sensitivity analysis results, and with simultaneous monitoring of stability factors, such as pore pressure variations, stability safety factors, and effect stress values. It is recommended that for each dam, a specific and tailored reservoir impounding plan be defined and implemented based on the physical and stability conditions of the dam after construction.

2. Resistance of rocks and sediments in the studied area

From the point of view of geology, the study area exhibits relatively gentle folding. Significant faults are located near this area, with the most notable being the Tabriz fault, which is situated south of the dam reservoir. The bedrock underlying the foundation areas and the dam axis consists of ultrabasic rocks from the Late Cretaceous period. The quality of the bedrock in this area ranges from poor to very poor. The weathering depth in the bedrock is significant, and there are numerous alteration and fracturing zones. A relatively thick cover of riverbed gravel overlays the bedrock. Figure 1 shows the map of the resistance of rocks and sediments in the studied area.

3. Main features of dam

The Madani rockfill Dam is built on the Aji Chai River in Tabriz, with a crown length of 277 m and a height of 91 m. The crown level of the dam is 1504 m, and the normal water level is 1498 m above sea level. The reservoir volume at the normal level is 361 $M \cdot m^3$. Excavation was carried out to a depth of 52 m in the riverbed to reach the bedrock. Two layers of fine- and coarse-grained filters are placed on both sides of the clay core to prevent the leaching of fine-grained materials from the clay core due to water flow through the dam body. The readings from these sensors have been continuously recorded since their installation. Figure 2 shows the plan of the Madani dam.

Table 1 presents the technical specifications of the Madani Dam and its reservoir (Ghods-Niroo Consultant Engineers Co., 2002a, 2002b, 2009, 2013).

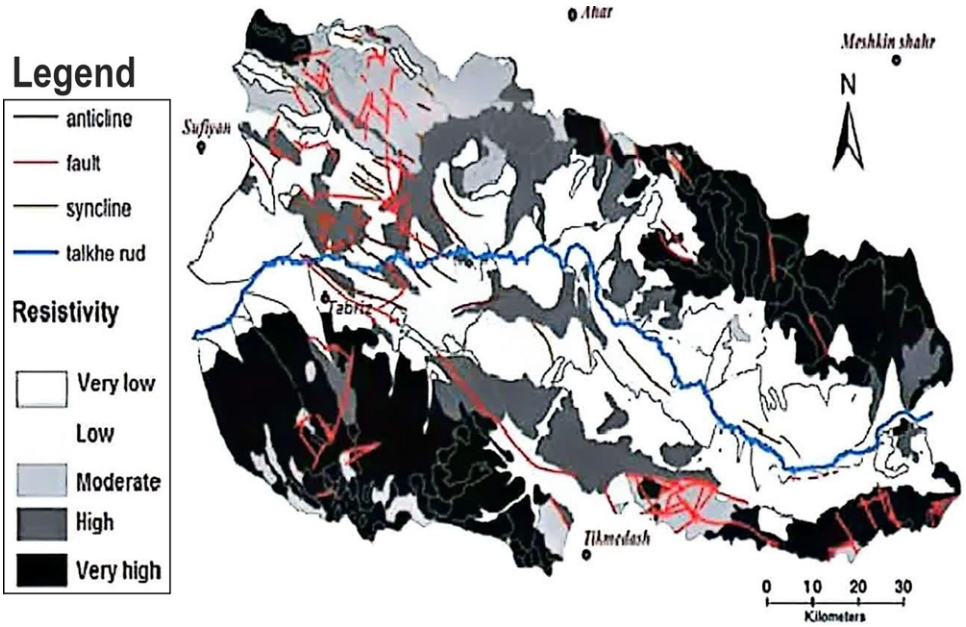

Figure 1. Map of the resistance of rocks and sediments in the studied area

Figure 2. Madani dam: plan view

Table 1. Technical specifications of the Madani dam and its reservoir

Dam detail	Value
Height of crest from bedrock (in the largest cross-section)	91 m
Height of crest from riverbed (in the largest cross-section)	39 m
Dam crest elevation	1504 m
Normal water level	1498 m
Length of dam crest	278 m
Width of dam crest	10 m
Total dam volume	361 M·m^3
Dam body materials volume	1.7 M·m^3
Dam slope up-stream	1: 2.3
Dam slope down-stream	1 : 2.1 + Berm
Total reservoir area	34.7 km

Dam stability was monitored by comparing changes over time to forecasts and existing standards. Based on the dam's characteristics and geological conditions, a monitoring system was implemented to control and manage the performance and behaviour of the Madani dam. Five sections of the dam body were instrumented to monitor the Madani dam during the design phase. Figure 3 shows the dam's longitudinal section and the largest cross-section.

All the data, including settlement, core pore pressure, and total stress, were collected from over 500 sensors installed in the dam body 10 years after its construction. A total of 120 pressure cells (PC), 62 piezoelectric sensors (VP), 27 piezometers (SP), 17 inclinometers (I), and 275 magnetic settlement detectors (SD) were installed in the dam body.

4. Material properties and numerical modelling

Three-dimensional (3D) dam bodies and supports were modelled using the Mohr–Coulomb behavioural model and the finite element software MIDAS-GTS.2019V2.1. MIDAS is specialised geotechnical software for analysing earth and rockfill dams, and its advantages include accurate modelling, straightforward analyses, and high computational speed.

4.1 Material properties

The mechanical properties of the materials used in the numerical analyses were obtained from soil mechanics laboratory tests. Table 2 lists the initial material parameters of the dam body based on the Mohr–Coulomb behaviour model.

In this table, the parameters, $\gamma_d\left(\frac{\mathrm{Kn}}{\mathrm{m}^3}\right)$, $\gamma_{sat}\left(\frac{\mathrm{Kn}}{\mathrm{m}^3}\right), K \times 10^{-6}\,(\mathrm{m/s})$, φ (deg), C (kPa), v, and E (MPa), are dry specific gravity, saturation specific gravity, permeability coefficient, internal friction angle, material adhesion, Poisson's ratio, and modulus of materials elasticity, respectively.

4.2 Modelling and analyses

3D modelling of the Madani Tabriz rockfill dam has been done using the Midas finite element software. Mohr–Coulomb elastoplastic behaviour model was used to introduce materials in numerical modelling. Triangular grids have been used for modelling (Vafaei *et al.*, 2023). The duration of the dam construction modelling is completely based on the reports received during the dam construction. Numerical modelling was carried out in three stages. At the start, the riverbed must be modelled to specify the residual stress of the bed. The horizontal stress values were calculated using the lateral pressure coefficient of the soil. In the second stage, excavation of the riverbed to reach the bedrock of the dam is modelled. Riverbed excavation modelling was done in ten layers. In the third stage, the numerical modelling of the dam body from the bedrock level to the riverbed level was carried out in ten layers; each layer was 6.4 m thick in the software. The construction operation took 6 years. Given the location of the river diversion tunnels, the underground water level will always be level with the riverbed. Considering the length of time of construction operations up to the riverbed and the high level of underground water in the area, the materials of the dam body are saturated below the level of the riverbed. The modelling of the riverbed to the crest of the dam (1504 m) was modelled in five layers. In this stage, the construction operation lasted about 3 years, and an undrained clay core was assumed. In stress analysis, the initial stress and the initial displacement of the support are considered zero. According to the results of sensitivity analysis, mesh size one is considered. Based on sensitivity analysis, horizontal and vertical boundary dimensions are selected to create the geometry. Figure 4 shows the 3D geometry mesh of the model.

5. Results and discussion

The results of the stress analysis, consolidation analysis, and the stability safety factor of the dam body at various reservoir impoundment levels are presented.

5.1 Settlement

The weight and density of materials during construction impose additional load on the underlying layers, leading to internal

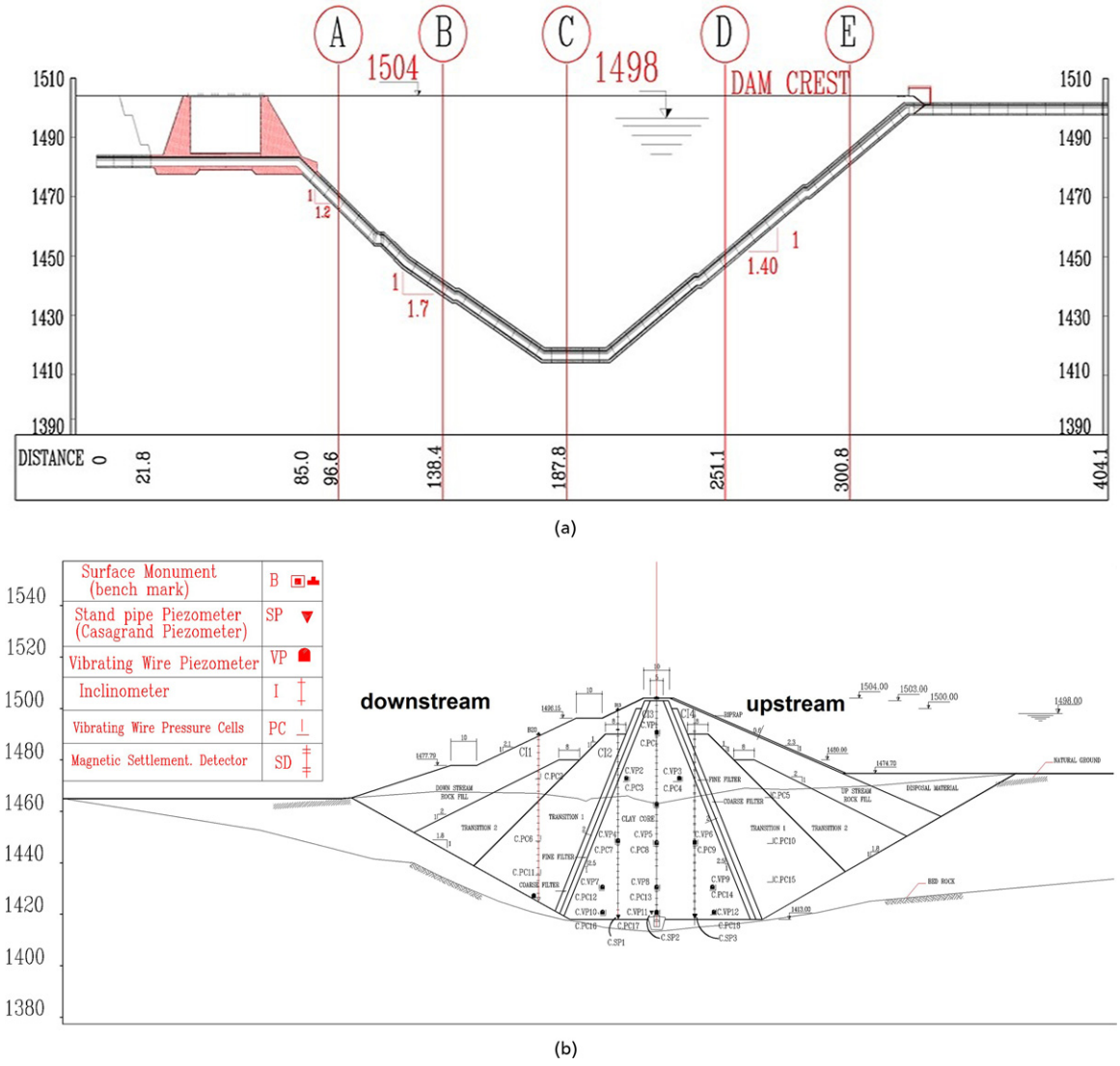

Figure 3. Madani dam: (a) dam longitudinal section and (b) largest cross-section

Table 2. List of the initial values material parameters dam body

Parameter	Clay core	Filter	Shell	Transient shell	Disposal	Alluvial foundation	Bed rock
γ_d	19	20	21	20	19.2	18.5	21
γ_{sat}	20	21	22	21	19.8	19.5	22
$K \times 10^{-6}$	0.05	10	100	100	10	100	0.001
φ	28	33	44	38	28	20	28
C	40	0	0	0	20	20	80
v	0.3	0.25	0.25	0.25	0.3	0.3	0.25
E	20	40	70	50	15	40	390

deformation. A series of magnetic plates were placed at different depths inside the settlement tube to measure the deformation of the dam body. The base plate was installed at the lowest level on the rock bed, where the least movement occurs, making this point nearly fixed. A total of 17 inclinometers and 275 magnetic settlement detectors were used at different levels of the dam body to assess the deformations of the Madani dam. Figure 5 shows the vertical settlement of the dam body resulting from the consolidation analysis.

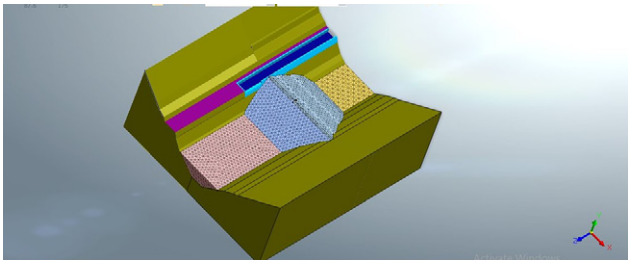

Figure 4. Madani dam: 3D geometry and mesh of the model

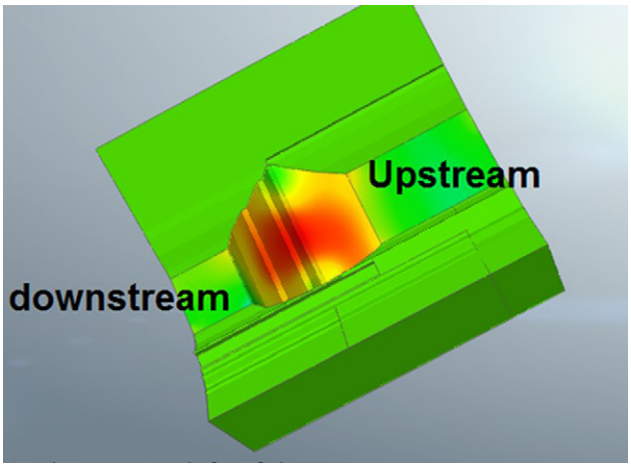

Figure 5. Contour of vertical settlement obtained from numerical analysis

In addition, Table 3 presents the vertical settlement values obtained from the magnetic settlement detectors and numerical analysis across five cross-sections of the dam.

The value of the settlement obtained from the data recorded by the precision tools is higher than the values obtained from the numerical analysis. Max vertical settlement 10 years after the end of construction of the Madani dam body, obtained from the monitoring data of precision instruments and numerical analysis, 1.90 and 1.79 m, respectively. The correlation coefficient of the settlement data obtained of the results from precision instruments and numerical analyses is more than 83.8%. Figure 6 shows the curve of settlement relative changes $\left(\frac{\Delta}{\Delta_{max}}\right)$ in cross-sections A, B, C, D, and E is shown to determine the dimensionless multivariate relationship between settlement, total stress, and pore water pressure.

Table 3. Maximum vertical settlement in cross-sections A, B, C, D, and E

Cross-section	A	B	C	D	E
Maximum settlement numerical analyses: m	0.45	1.55	1.79	1.3	1.1
Maximum settlement instruments: m	0.469	1.56	1.9	1.33	1.17

In Figure 6, H is the level at which settlement was measured (level of settlement plates), H_{max} is the maximum dam crown level, Δ is the settlement, and Δ_{max} is the maximum settlement.

5.2 Vertical stress

Pressure cells are tools that record changes in the total stress in different parts of the dam body. In Madani Dam, 120 pressure cells are installed in different body parts. Pressure cells measure stresses in three directions (two horizontal directions and one vertical direction). Table 4 shows the total vertical stress value obtained from pressure cells and numerical analysis.

In Table 4, PC is the vibrating wire pressure cell that was installed in five different cross-sections of the dam. The total stress value in the pressure cells is lower than the value obtained from the numerical analysis. Because there is less density around the cell than other parts of the core to prevent damage. The maximum vertical stress occurs at the centre of the core. The maximum value of the total stress obtained from pressure cells and numerical analysis at the junction of the core to the foundation is 1205 and 1440 kPa, respectively. The correlation coefficient between the total stress data obtained from the instrumentation and numerical analyses is 99.09%.

Figure 7 shows the stress change curves $\left(\frac{\sigma}{\sigma_{max}}\right)$ and the correlation coefficient between the data obtained from the results of pressure cells and numerical analysis.

In Figures 7, H is the level of the plates, H_{max} is the maximum dam crown level, σ is stress, and σ_{max} is the maximum stress.

5.3 Pore water pressure

In Madani Dam, electric piezometers and Casagrande have been used to determine the pore pressure. Regarding the large width of the clay core, the presence of overburden, the low permeability of the core, and proper compaction, additional pore pressure has been created in the dam body. The maximum pore water pressure created 10 years after the end of construction has been observed in the lower levels and the middle part of the clay core (the place where the core is connected to the foundation). Table 5 shows the values of pore water pressure in sections C, B, and D obtained from electric piezometers (VP), Casagrande piezometers (SP), and numerical analysis.

The maximum values of pore water pressure obtained from piezometers and numerical analysis are 420 and 450 kPa, respectively. Due to the passage of time and proper consolidation of the core material, there is a very good fit between the data. The correlation coefficient between the pore pressure data obtained from piezometer results and numerical analysis is 67.31%. The value of Ar, the arching ratio obtained from the monitoring of precision instrument data, and the results of numerical analysis are 0.35 and 0.47, respectively, which are close to the

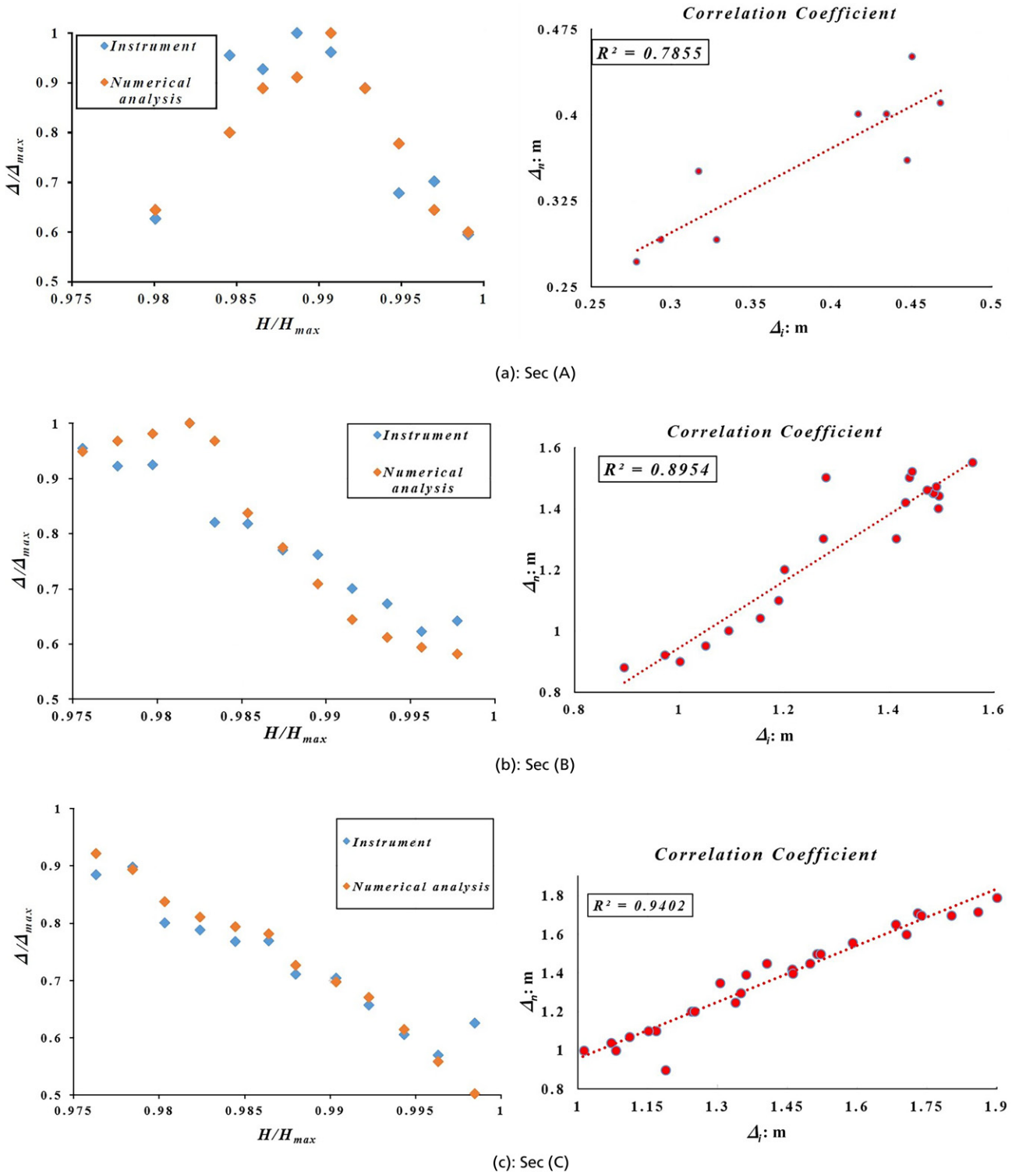

Figure 6. Settlements curves comparison and correlation coefficients in cross-sections A, B, C, D, and E

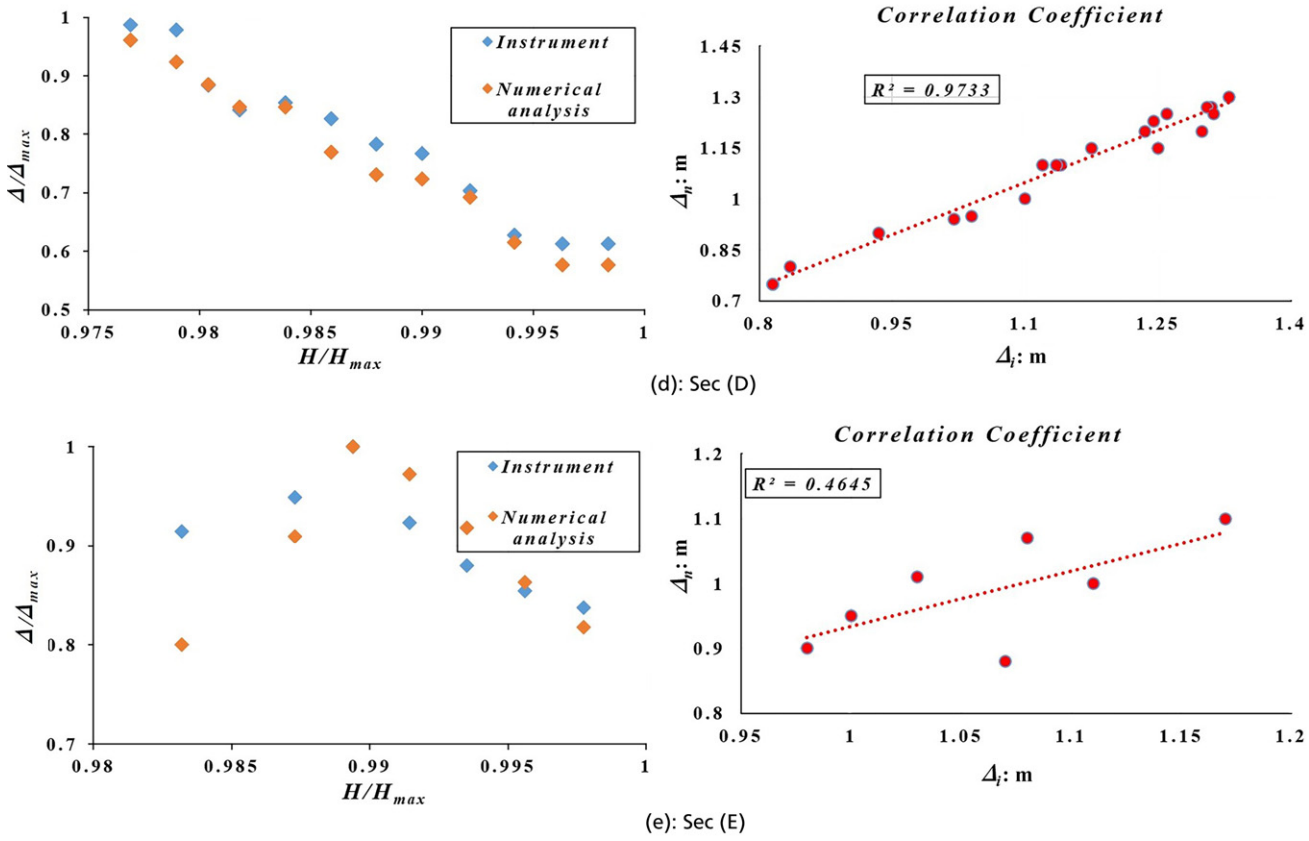

Figure 6. Continued

value of the design stage (0.5). The likelihood of arching and hydraulic failure due to the value of the arcing ratio and the large width of the core is not possible. After impounding, due to the water pressure on the upstream of the dam, the arching ratio must be checked because if the value of this ratio is small at the end of the construction, the possibility of arching to occur is very high. Figure 8 shows the change curve $\left(\frac{P}{P_{\max}}\right)$ obtained from electric piezometers, and the correlation coefficient between the data obtained from the results of pressure cells and numerical analyses are presented.

In Figures 8, H is the plate level, $H_{\max}$ is the maximum dam crown level, ρ is the pore water pressure, and $\rho_{\max}$ is the maximum pore water pressure.

In this section, we used 27 data with a correlation coefficient above 89%. Multivariate regression presented a relationship between the relative changes of the settlement (dependent variable) based on the relative changes of the pore water pressure and the total stress.

Equation 1 shows the relation of relative changes of the settlement.

1. $$Y = \frac{\Delta}{\Delta_{max}} = f\left(\frac{\sigma}{\sigma_{max}}, \frac{\rho}{\rho_{max}}\right)$$

2. $$Y = \frac{\Delta}{\Delta_{max}} = 0.807 - 0.0011795\left(\frac{\sigma}{\sigma_{max}}\right) - 0.0582\left(\frac{\rho}{\rho_{max}}\right)$$

where Y is the relative changes of settlement to maximum settlement (dependent variable), $\left(\frac{\sigma}{\sigma_{\max}}\right)$ is the relative changes of stress to maximum stress (independent variable), and $\left(\frac{P}{P_{\max}}\right)$ is the relative pore pressure changes to maximum pore water pressure (independent variable).

5.4 Reservoir impounding programme

Due to the special conditions of the Madani rockfill dam, where the construction of the dam body took 10 years and another 10 years have passed since its completion, the reservoir impounding process will not follow conventional procedures. Therefore, a safe and specialised impounding plan for the Madani rockfill dam must be developed based on the dam's specific conditions,

Table 4. Vertical stresses in cross-sections A, B, C, D, and E

Cell no.	Location	Distance to axis: m	Install elevation: z	Vertical total stress: kPa	
				Instruments	N. analyses
APC.1	Core centre	0.74	1490.070	181	213
APC.2	Down-stream core	−6.685	1475.366	365	460
APC.3	Up-stream core	6.754	1475.9	351	445
BPC.1	Core centre	0.075	1490.1	189	234
BPC.3	Down-stream core	−9.546	1469.794	419	559
BPC.4	Up-stream core	10.302	1469.794	413	552
BPC.7	Down-stream core	−17.061	1454.338	565.0	790
BPC.8	Core centre	0.36	1454.457	615.0	820
BPC.9	Up-stream core	18.025	1454.489	580	800
BPC.11	Down-stream core	−16.2	1439.205	805	1095
BPC.12	Core centre	0.08	1439.164	880	1120
BPC.13	Up-stream core	16.81	1439.161	845	1100
CPC.1	Core centre	0.5	1490.11	192.4	240
CPC.3	Down-stream core	−10.541	1470.036	430	583
CPC.4	Up-stream core	10.245	1469.935	419.3	579
CPC.7	Down-stream core	−16.926	1454.649	575.0	805
CPC.8	Core centre	0.492	1454.66	630.18	845
CPC.9	Up-stream core	17.957	1454.629	591.62	812
CPC.12	Down-stream core	−20.023	1430.909	1008.3	1250
CPC.13	Core centre	0	1431	—	1270
CPC.14	Up-stream core	20.312	1431.321	1070.5	1255
CPC.16	Down-stream core	−20.43	1420.294	1205	1425
CPC.17	Core centre	0121	1420.55	1150	1440
CPC.18	Up-stream core	19.841	1420.296	1160	1420
DPC.1	Core centre	0.4	1490.11	184	226
DPC.3	Down-stream core	−10.692	1470.11	417	551
DPC.4	Up-stream core	10.779	1470.159	408	544
DPC.9	Down-stream core	−17.917	1454.422	560.0	785
DPC.10	Core centre	0.352	1454.488	605.0	820
DPC.11	Up-stream core	17.965	1454.17	575	790
DPC.6	Down-stream core	−17.15	1439.158	790	1080
DPC.7	Core centre	0.18	1439.044	850	1100
DPC.8	Up-stream core	17.07	1439.129	822	1070
EPC.1	Core centre	0.049	1489.96	175	204
EPC.2	Down-stream core	−6.88	1479.846	345	411
EPC.3	Up-stream core	6.73	1479.907	321	404

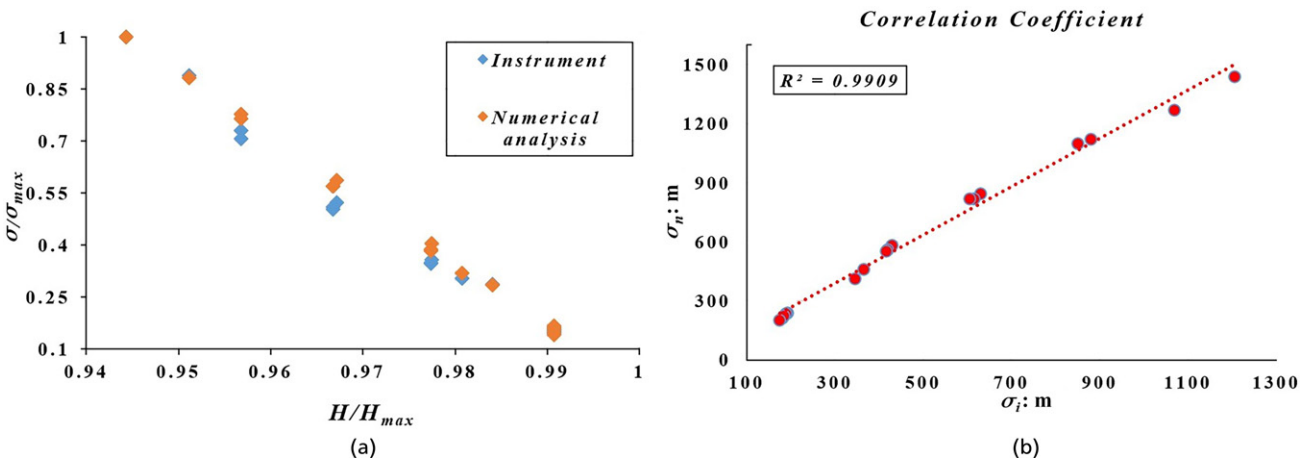

Figure 7. (a) Vertical total stress changes and (b) correlation coefficient between precision instruments and numerical analysis values of total stress

Table 5. Values of pore water pressure in cross-sections B, C, and D

Piezometer no.	Location	Distance axis: m	Install elevation: z	Pore pressure		r_u		R_u	
				Instruments	N. analysis	Instruments	N. analysis	Instruments	N. analysis
BVP.7	Down-stream core	−17.36	1439.18	358.6	375	0.27	0.28	0.44	0.34
BVP.8	Core centre	0.48	1439.16	360.2	380	0.27	0.28	0.4	0.33
BVP.9	Up-stream core	16.49	1439.22	366.5	385	0.28	0.29	0.43	0.35
BSP.1	Down-stream core	−15	1438	175	380	0.13	0.28	—	0.34
BSP.2	Core centre	−3.19	1438	161	383	0.12	0.28	—	0.33
BSP.3	Up-stream core	13.38	1437	195	395	0.14	0.29	—	0.35
CVP.10	Down-stream core	−20.6	1420.52	340	402	0.2	0.24	0.28	0.282
CVP.11	Core centre	0.422	1420.58	328	396	0.19	0.23	0.28	0.27
CVP.12	Up-stream core	20.25	1420.29	347	414	0.2	0.24	0.29	0.29
CSP.1	Down-stream core	−16.24	1416.7	403	438	0.22	0.25	—	0.29
CSP.2	Core centre	−3.80	1416.7	392	425	0.22	0.24	—	0.28
CSP.3	Up-stream core	15.9	1416.7	420	450	0.23	0.25	—	0.3
DVP.4	Down-stream core	−16.42	1439.14	377.7	355	0.28	0.27	0.47	0.32
DVP.5	Core centre	0.12	1439.02	352	363	0.26	0.275	0.4	0.33
DVP.6	Up-stream core	17.1	1439.1	361.1	380	0.27	0.28	0.43	0.35
DSP.1	Down-stream core	−14.91	1438	96	358	0.07	0.27	—	0.33
DSP.2	Core centre	−2.92	1439	86	363	0.06	0.275	0.1	0.33
DSP.3	Up-stream core	14.85	1439	86	380	0.06	0.28	0.1	0.35

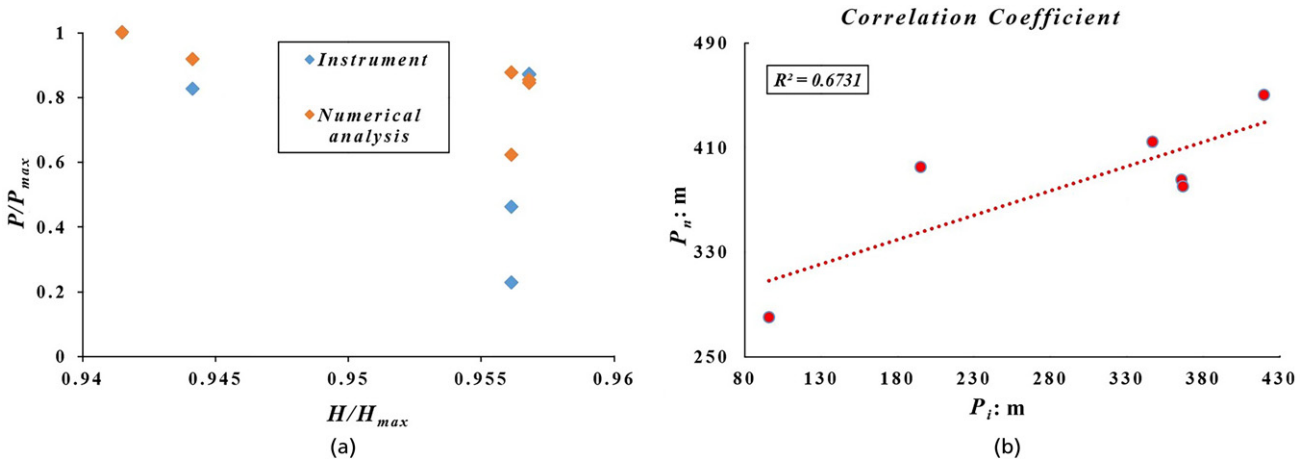

Figure 8. (a) Pore pressure changes and (b) correlation coefficient between numerical and experimental values of pore pressure

including sensitivity analyses that involve numerical stability analyses assuming reservoir impounding at different levels. Simultaneous monitoring of key stability factors, such as impounding time, pore water pressure, stability safety factors, and effective stress, is essential. Furthermore, it is necessary to maintain appropriate monitoring of the dam's stability during the reservoir impounding and operational phases by using data from settlement gauges, inclinometers, pressure cells, and electric piezometers installed at five cross-sections of the dam body. Based on this approach, it is recommended that for any dam that has not yet been impounded or is still under construction, a specialised impounding plan tailored to the specific conditions of that dam, including the construction period and other factors affecting dam stability, should be developed. Figures 9 and 10 show the dam body stability factors considering the time and different impounding levels, respectively. Figure 11 illustrates the changes in effect stress based on different reservoir impounding levels.

Figure 10 shows that the dam reservoir can be fully impounded in 80 d with a controlled filling rate of 30 cm/d. As the reservoir is filled, the clay cores become saturated, and water is expelled from the clay cores during this period. Under these conditions, the pore water pressure in the core and the dam body's stability factor remain within acceptable limits. When the water level in the reservoir rises, the rate of pore pressure increase in the core slows down, and the rate of effect stress reduction decreases. In

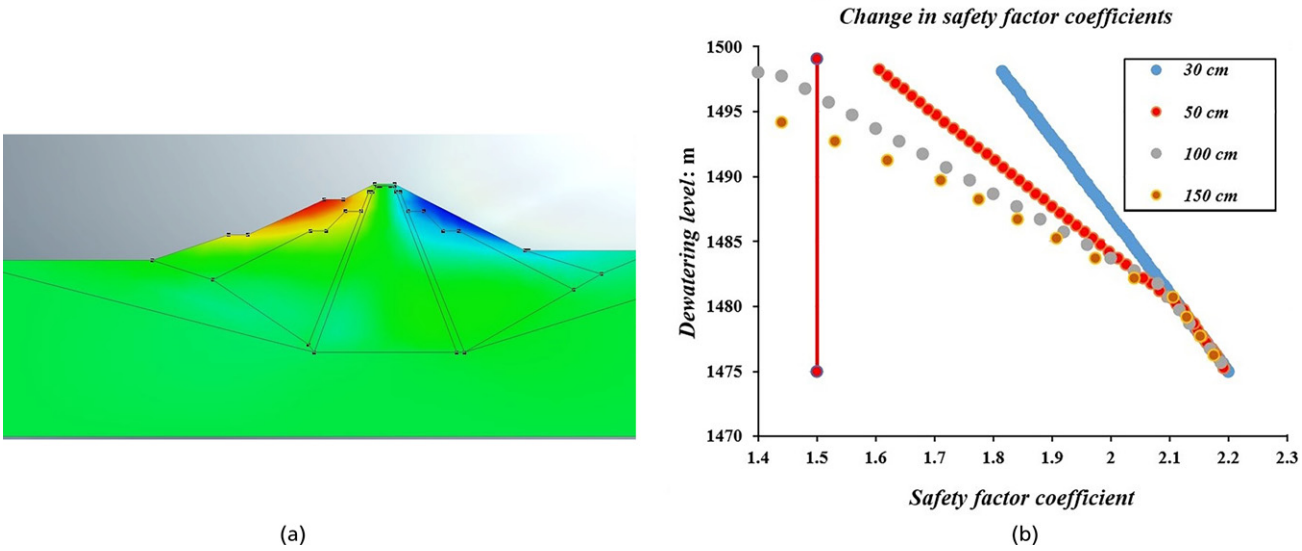

Figure 9. (a) Changes factor of safety and (b) levels of impounding the dam reservoir

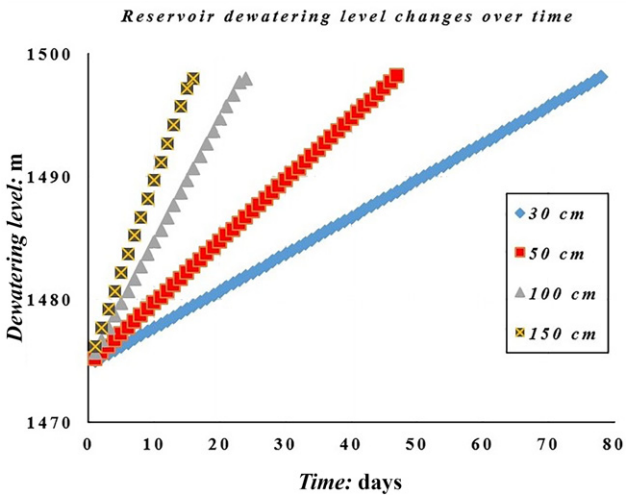

Figure 10. Changes in reservoir level of dam based period time

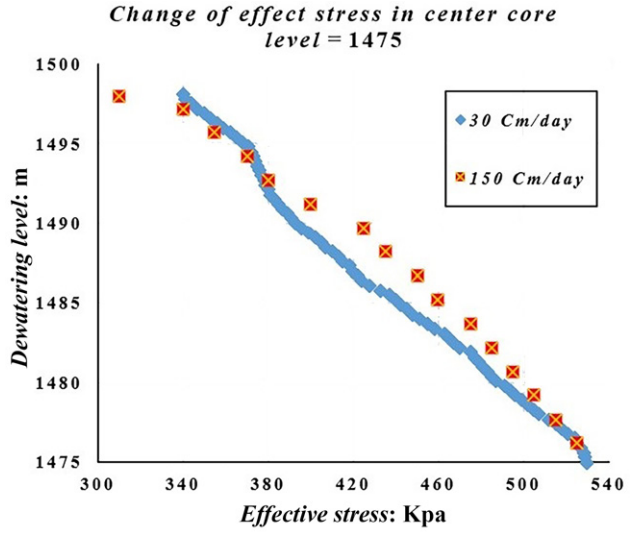

Figure 11. Variation of effective stress and levels of impounding the reservoir of the dam

Figure 11, the changes in pore water pressure and effect stress in the core at two filling rates, 30 and 150 cm/d, are compared. Sensitivity analyses of the impounding process were conducted, and it is recommended that the reservoir be filled at a rate of 30 cm/d.

6. Conclusion

Max vertical settlement, based on instrumentation readings and numerical analyses, is 190 cm and 179 cm, respectively. The maximum vertical stress at the core-foundation interface, obtained from pressure cell readings and numerical analysis, is 1205 and 1440 kPa, respectively. The maximum pore water pressure recorded by installed piezometers and from numerical analysis is 420 and 450 kPa, respectively. The correlation coefficients between the instrument data and numerical analysis results for total stress, pore pressure, and settlement are 99.09, 67.31, and 83.8, respectively. The results indicate a very strong correlation between the numerical and experimental data. It is recommended to control the impounding rate of the reservoir to prevent increased pore water pressure during the impounding process and to avoid hydraulic failure. Based on the instrumentation data for the Madani dam body and numerical analysis results, it can be

concluded that the dam's instrumentation system provides accurate measurement and recording. The impounding of the reservoir for this specific dam should not be carried out solely based on conventional codes. Sensitivity analysis of the reservoir impounding at different levels until reaching the normal reservoir level was conducted. For this particular dam, given that 10 years have passed since the dam body was completed, with a maximum impounding rate of 30 cm/d, pore pressure in the core can be controlled, and by monitoring the stability safety factor and effective stress, the reservoir will be safely filled within 80 d. Therefore, it is recommended that for each earth or rockfill dam, a specific impounding plan should be developed, considering all safety aspects of the dam.

REFERENCES

Behrouz Sarand F, Dibamehr A and Vafaeipoor R (2023) Improvement of Tabriz green marl using alkaline activated zeolite and metaclay. *Journal of Civil and Environmental Engineering*, https://doi.org/10.22034/CEEJ.2023.54867.2213.

Beiranvand B and Komasi M (2019) Monitoring and numerical analyses of pore water pressure changes Eyvashan dam during the first dewatering period. *Journal of Applied Research in Water and Wastewater* **6(11)**: 1–7, https://doi.org/10.22126/ARWW.2019.1017.

Blind H (1983) The safety of dams. *Water Power and Dam Construction* **35(5)**: 17–21.

Cheng L, Tong F, Li Y, Yang J and Zheng D (2021) Comparative study of the dynamic back-analyses methods of concrete gravity dams based on multivariate machine learning models. *Journal of Earthquake Engineering* **25(1)**: 1–22, https://doi.org/10.1080/13632469.2018.1452802.

Farajniya R, Poursorkhabi RV, Zarean A and Dabiri R (2022) Investigating the arching in Rock-Fill dam ten years after the end of construction using numerical analyses and monitoring. *Ferdowsi Civil Engineering* **35(1)**: 59–74, https://doi.org/10.22067/JFCEI.2022.73934.1098.

Ghaemi A and Konrad JM (2022) Empirical approaches to estimate the nonlinear dynamic responses of earth-core rock fill dams subjected to earthquake ground motions. *Soils and Foundations* **62(2)**: 101106, https://doi.org/10.1016/j.sandf.2022.101106.

Ghanbari A and Shams RS (2015) Development of an empirical criterion for predicting the hydraulic fracturing in the core of earth dams. *Acta Geotechnica* **10(2)**: 243–254, https://doi.org/10.1007/s11440-013-0263-2.

Ghiasi V, Heydari F and Behzadinezhad H (2021) Numerical analyses and back calculation for embankment dam based on monitoring results (case study: Iran-Lurestan Rudbar). *Scientia Iranica*, https://doi.org/10.24200/SCI.2021.56159.4579.

Ghods-Niroo Consultant Engineers Co (2002a) *Geological Report of Madani Dam Engineering, Tehran*. Ghods-Niroo Consultant Engineers Co.

Ghods-Niroo Consultant Engineers Co (2002b) *Technical Report on the Studies of the Second Phase of Madani Dam, Tehran*. Ghods-Niroo Consultant Engineers Co.

Ghods-Niroo Consultant Engineers Co (2009) *Technical Review of Numerical Analyzes to Control the Static and Dynamic Stability of Madani Dam, Tehran*. Ghods-Niroo Consultant Engineers Co.

Ghods-Niroo Consultant Engineers Co (2013) *Technical Report on the Instrumentation of the Body of Madani Dam, Tehran*. Ghods-Niroo Consultant Engineers Co.

Guo X, Baroth J, Dias D and Simon A (2018) An analysical model for the monitoring of pore water pressure inside embankment dams. *Engineering Structures* **160**: 356–365, https://doi.org/10.1016/j.engstruct.2018.01.054.

Khalili-Maleki M, Poursorkhabi RV, Nadiri AA and Dabiri R (2022) Prediction of hydraulic conductivity based on the soil grain size using supervised committee machine artificial intelligence. *Earth Science Informatics* **15(4)**: 2571–2583, https://doi.org/10.1007/s12145-022-00848-x.

Komasi M and Beiranvand B (2019) Evaluation of pore water pressure foundation and core of Sivand dam after the first dewatering period in comparison with the actual instrument results. *Journal of Iranian Dam and Hydroelectric Power Plant* **6(21)**: 66–73. http://journal.hydropower.org.ir/article-1-304-en.html.

Komasi M, Mazaheri AR and Beiranvand B (2019) Numerical analyses of the arching effect of Ayoshan dam in the first dewatering period and its comparison with accurate instrument results. *Journal of Water and Soil Conservation Research* **26(6)**: 79–97, https://doi.org/10.22069/JWSC.2019.14530.2969.

Liu S, He W, Sun Y, Shen C and Wang L (2023) Analyses of the behavior of a high earth-core rock fill dam considering particle breakage. *Computers and Geotechnics* **157**: 105320.

Mazaheri AR, Alipour R and Shokri Derivand B (2020) Study the monitoring and numerical analyses of Rock Fill dam (case study of Marvak dam in Lorestan, Iran). *Civil Infrastructure Researches* **5(2)**: 153–164, https://doi.org/10.22091/cer.2020.5223.1194.

Rashidi M and Haeri SM (2017) Evaluation of behaviors of earth and rock fill dams during construction and initial impounding using instrumentation data and numerical modeling. *Journal of Rock Mechanics and Geotechnical Engineering* **9(4)**: 709–725, https://doi.org/10.1016/j.jrmge.2016.12.003.

Sivasuriyan A, Vijayan D, Munusami R and Devarajan P (2021) Health assessment of dams under various environmental conditions using structural health monitoring techniques: a state-of-art review. *International Research on Sustainable Developments for Environment Management*: 455–464, https://doi.org/10.1007/s11356-021-16749-3.

Soroush A and Aghaei Araei A (2006) Analyses of behaviour of a high rock fill dam. *Proceedings of the Institution of Civil Engineers – Geotechnical Engineering ICE Virtual Library* **159(1)**: 49–59, https://doi.org/10.1680/geng.2006.159.1.49.

Vafaei PR, Zareh A, Alizadeh Majdi A and Behrouz Sarand F (2023) Investigating the efficiency of modified element-free Galerkin method in solving static problems and optimization. *Analyses of Structure and Earthquake* **20(3)**: 26–34, https://doi.org//10.30495/civil.2023.706890.

Zareh A, Poursorkhabi RV, Majdi AA and Sarand FB (2023) The efficiency of the electro-osmosis method on the consolidation and strength properties of the gray clay of tabriz. *Geoenvironmental Disasters* **10(1)**: 16, https://doi.org/10.1186/s40677-023-00245-6.

Zhenyu W, Chen C, Xiang L, Liang P and Limin Z (2020) Discussion on the allowable safety factor of slope stability for high Rock fill dams in China, Journal of Elsevier. *Engineering Geology* **272**: 105666–105235, https://doi.org//10.1016/j.enggeo.2020.105666.

Zhou W, Hua J, Chang X and Zhou C (2011) Settlement analyses of the Shuibuya concrete-face Rock fill dam. *Comp. and Geot* **38**: 269–280, https://doi.org//10.1016/j.compgeo.2010.10.004.